

Effect of lattice instability on superconductivity in sodium tungsten bronze

K. L. Ngai

Naval Research Laboratory, Washington, D.C. 20375

Richard Silbergliitt

National Science Foundation, Washington, D.C. 20550

(Received 4 November 1974)

The effect of lattice instability on the electronic properties of the tungsten bronzes, $M_x\text{WO}_3$ ($0 < x < 1$), is considered. A model of the free energy which describes the various phases as local minima in configuration space is shown to provide a basis for understanding the structures observed and transformations between them when M is an alkali metal. For the case of Na_xWO_3 , the effect on the superconducting transition temperature of a phonon which is assumed to soften as a function of x is explicitly calculated. Tunneling between the local free-energy minima is assisted by this soft phonon. Good agreement is obtained with recent experimental observations of a dramatic increase in T_c as x decreases and approaches the critical value for transition between the superconducting and semiconducting tetragonal phases. Noteworthy features of this work are that the structural transformation does not correspond to a simple condensation of the soft phonon, and also that the phonon softening and configurational tunneling are considered simultaneously.

I. INTRODUCTION

The tungsten bronzes are a class of nonstoichiometric compounds with the formula $M_x\text{WO}_3$ ($0 < x < 1$), which are known to exist in cubic, hexagonal, and two different tetragonal structures.¹ Some of these materials have been found to be superconducting² in the hexagonal and one of the tetragonal structures, and recently an increase in the superconducting transition temperature of the higher composition tetragonal sodium tungsten bronze has been observed as x is decreased toward the value at which the transition to the lower composition tetragonal structure occurs.³ It was suggested in Ref. 3 that this increase is due to softening of the lattice mode which corresponds to a certain geometrical operation⁴ that transforms one tetragonal structure into the other. In this paper we will introduce a simple model of the composition dependence of the free energy and the soft-phonon frequency, from which the observed dependence of T_c on x can be obtained. The structural transition is treated as a change in bonding configurations, so that the model is similar to the two-well configuration-space model utilized recently⁵ to treat amorphous materials. In the present case the tunneling between configurations is assisted by the soft phonon, which is itself treated in a generalization of the anharmonic model⁶ of lattice instabilities. We find that as x is decreased toward x_c , the critical composition for transition between structures, the phonon softening at first strongly enhances T_c . Near x_c however, the coupling between the soft phonon and the configuration change suppresses the softening, and T_c increases more slowly. In this simple model, then the effect of the soft phonon on T_c is explicitly calculated for a system where the

superconducting and structural transitions can occur simultaneously.

II. MODEL

For values of x in the upper portion of the range $0 < x < 1$, many of the tungsten bronzes take on a cubic perovskite-related structure. The matrix of WO_6 octahedra for this structure is shown in Fig. 1. The M atoms (not shown) would occupy the body centered position in the cubic unit cell. For very small values of x , a tetragonal structure with very few M atoms present is found. The matrix of WO_6 octahedra for this structure is illustrated in Fig. 2(a), where a view in the a - b plane is shown. The other tetragonal structure is shown in Fig. 2(b).

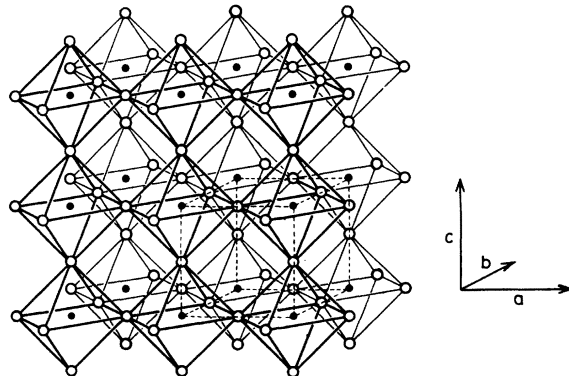


FIG. 1. Matrix of WO_6 octahedra for the cubic perovskite-related structure of $M_x\text{WO}_3$. Open circles represent O atoms, filled circles W atoms. M atoms (not shown) would occupy the body centered position in the cubic unit cell.

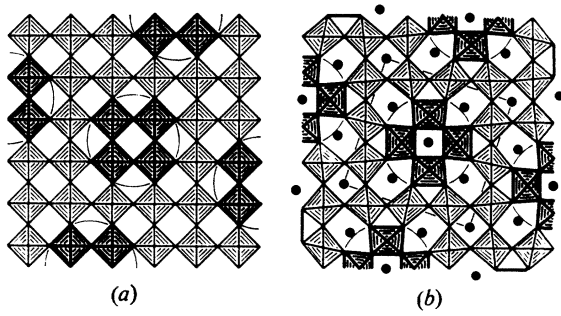


FIG. 2. (a) Matrix of WO_6 octahedra in $T2$ structure, projected on a - b plane. (b) Matrix of WO_6 octahedra in $T1$ structure. Circles identify groups of octahedra which have been rotated by 45° to change (a) to (b). Filled circles represent M atom sites, not necessarily all occupied.

There exists a simple geometrical operation⁴ which takes one between the two tetragonal structures. This operation consists of the rigid rotation of each of the groups of four circled WO_6 octahedra by 45° about the center of the unit. Hereafter we refer to the rotated structure as $T1$ [Fig. 2(b)] and the simple tetragonal structure as $T2$ [Fig. 2(a)]. The M atoms occupy the "tunnels" between the arrays of WO_6 octahedra, so that the essential difference between $T1$ and $T2$ is the replacement of eight square tunnels by four pentagonal ones and four triangular ones per unit cell. Note that by rotating neighboring groups of octahedra one can form hexagonal tunnels as well, so that many other structures in addition to $T1$ can be obtained from $T2$, as pointed out in Ref. 4. The stability of a particular structure will depend upon the free energy of the M atoms in the tunnels found in that structure. For example, if M is sodium, one might expect that the sodium atoms would prefer the larger pentagonal tunnels, since the Na-O distance in the square tunnels is only 1.95 \AA ,⁷ whereas the Na-O bond length in NaWO_3 is 2.73 \AA .⁸ One may take this effect into account by writing the free energy for a given configuration $\{\vec{r}_i\}$ of the octahedra as

$$F\{\vec{r}_i\} = W\{\vec{r}_i\} + N \sum_{\alpha} n_{\alpha}\{\vec{r}_i\} M_{\alpha}, \quad (1)$$

where α is summed over square, triangular, pentagonal, and hexagonal tunnels, N is the total number of (square) tunnels in the $T2$ structure, $n_{\alpha}\{\vec{r}_i\}$ is the fraction of occupied α -type tunnels in the $\{\vec{r}_i\}$ configuration, M_{α} is the free energy of the M atom in an α -type tunnel, and $W\{\vec{r}_i\}$ is the free energy of the WO_6 octahedra, connected as in configuration $\{\vec{r}_i\}$, and in the absence of M atoms. Now $F\{\vec{r}_i\}$ is to be minimized with respect to the constraint:

$$\sum_{\alpha} n_{\alpha}\{r_i\} = x. \quad (2)$$

We note that the M_{α} will depend strongly on the size of M . A small atom such as lithium will be easily accommodated in the square tunnels. However, for an atom as large as rubidium one would expect the free energy in the hexagonal configuration to be the lowest. Comparing the M -O bond lengths⁸ found in similar compounds with the size of the various tunnels,⁷ one can understand qualitatively the occurrence⁹ (under ordinary conditions) of the lithium tungsten bronze in only the cubic and $T2$ structures. This fact is due to the small reduction in energy

$$N \sum_{\alpha} n_{\alpha}\{T1\} M_{\alpha} - N \sum_{\alpha} n_{\alpha}\{T2\} M_{\alpha}$$

for Li, which cannot compensate for the larger increase in the WO_6 octahedra configurational energy, $W\{T1\} - W\{T2\}$. Similar reasoning explains why sodium tungsten bronze occurs only in cubic, $T1$ and $T2$ structures, the potassium in cubic, $T1$, $T2$, and hexagonal, and the rubidium in only hexagonal. Moreover, from the constraint Eq. (2) one sees that $T1$ cannot be stable for¹⁰ $x > 0.6$ and that the hexagonal phase¹¹ cannot be stable for $x > 0.33$.

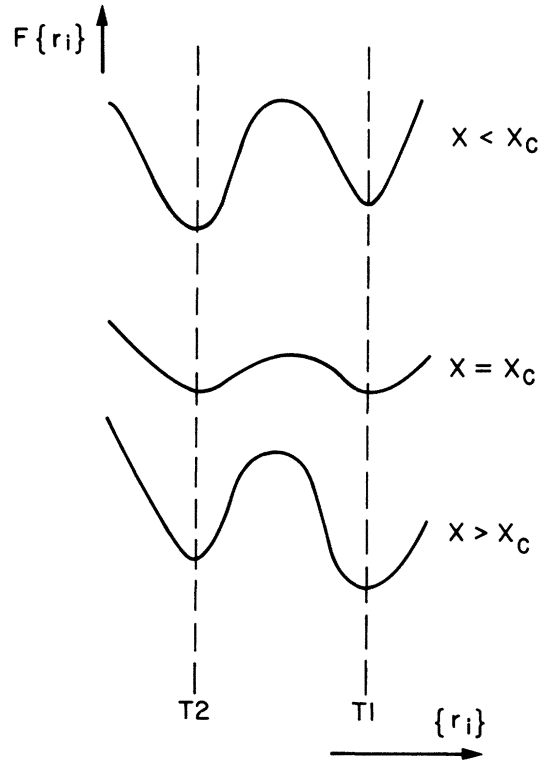


FIG. 3. Compositional dependence of the configurational free energy, $F\{\vec{r}_i\}$. The ordered phases $T1$ and $T2$ shown in Fig. 2 are local minima. Intermediate configurations are represented schematically as a quantum barrier. The rotational modes depicted in Fig. 2 correspond to specific excursions about the local minima in $F\{\vec{r}_i\}$.

For the remainder of this paper we will focus our attention on the sodium tungsten bronze. In this case, $M_p < M_s \ll M_t$. The triangular tunnels are so small that n_t can be neglected. Thus the free energy takes the form

$$F\{T1\} = W\{T1\} + N[n_s\{T1\}M_s + n_p\{T1\}M_p] \\ (n_s + n_p = x), \quad (3a)$$

$$F\{T2\} = W\{T2\} + NxM_s, \quad (3b)$$

where $W\{T2\} < W\{T1\}$. For small values of x , $T2$ is clearly the stable structure, since the increase in W energy will not be compensated by the M terms in Eq. (3). However, as x increases, the energy lowering obtained by increasing n_p and decreasing n_s will at some point (x_c) compensate the difference $W\{T1\} - W\{T2\}$, as illustrated in Fig. 3. For values of $x > x_c$, but less than $x \sim 0.6$, $T1$ should be the stable structure. Experimentally, x_c is found⁹ to be about 0.2, and x_{\max} about 0.5. To complete the model, we note that the rotation shown in Fig. 2 takes one from $T2$ to $T1$ and vice versa. However, the change in configurations requires the breaking of both $W-O$ and $M-O$ bonds, so that the transition does not result from a simple condensation of the phonon mode corresponding to the rotation. It follows, however, from the fact that $F\{\vec{r}_i\}$ is linear in x that this phonon frequency will soften in the manner

$$\omega_0^2 = c^2(x - x_0) \quad (4)$$

as x approaches x_c .¹² Physically this corresponds to the weakening of the force constants for the rotational mode as the M atoms are depleted from the pentagonal tunnels. x_0 is expected to be greater than zero, since the rotation should be unstable at $x=0$, when $T2$ is by far the low free-energy configuration.

A general physical argument can be made in favor of compositionally-dependent mode softening in "cage" or "tunnel" structures. Such structures are characterized by holes in the lattice, a certain number of which are filled at any given composition. In the limit of low concentration (many empty holes), one might expect to find low-frequency modes corresponding to the motions of the large groups of atoms surrounded by the holes, and thus effectively decoupled from the rest of the lattice. As the concentration of the atoms which fill the holes is increased, these motions become restricted, the lattice becomes stiffer, and the phonon mode frequencies are no longer especially low. This is precisely the effect which we are attempting to describe in Na_xWO_3 with Eq. (4). This is analogous to the usual anharmonic soft mode case,⁶ with two notable differences. In contrast to the anharmonic case, in this system one may obtain a softening even in the harmonic approximation.¹² Also, the

parameter which determines the phonon frequency is the M concentration rather than the temperature.

III. PHONON-CONFIGURATION COUPLING

As one approaches x_c , the two wells in $F\{\vec{r}_i\}$ will be close in energy, and tunneling between configurations may occur, assisted by the ω_0 phonon. In fact, electron-microscope pictures of alkali tungsten bronzes¹³ show that local regions of $T2$ structure are sometimes embedded within a large $T1$ matrix. The effect of this tunneling process on the phonon frequency will now be considered. For this purpose we treat the two configurations as a pseudo-spin- $\frac{1}{2}$ system and use the following model Hamiltonian:

$$H = \omega_0 a^\dagger a + \nabla E S^z + V(x) (S^+ a^\dagger + S^- a), \quad (5)$$

where ω_0 is given by Eq. (4), $\Delta E = \epsilon(x - x_c)$ is the difference between the free energies of the $T1$ and $T2$ configurations (assumed to be linear in x), and $V(x)$ is the matrix element for the configuration tunneling.¹⁴ This matrix element, which increases as x approaches x_c due to the flattening of the $T1$ well as ω_0 softens, is assumed to have the form $V(x) = V_0 \exp[-\xi(x - 0.2)]$. The effect of the configuration coupling term on the phonon frequency may be obtained from the phonon self-energy,¹⁵ according to

$$\Sigma_{ph}(\omega) = \frac{V^2(x)}{\omega - \epsilon(x - x_0) + i\delta}, \quad (6)$$

which gives for the phonon propagator¹⁵ ($\omega > 0$)

$$D(\omega) = \left(\omega - c(x - x_0)^{1/2} - \frac{V^2(x)}{\omega - \epsilon(x - x_c)} + i\delta \right)^{-1}. \quad (7)$$

Thus

$$D(\omega) = \frac{\omega - \epsilon(x - x_c)}{(\omega - \omega_+)(\omega - \omega_-) + i\delta} \quad (8)$$

where

$$\omega_{\pm} = \frac{1}{2} [c(x - x_0)^{1/2} + \epsilon(x - x_c)] \pm \frac{1}{2} \{ [c(x - x_0)^{1/2} - \epsilon(x - x_c)]^2 + 4V^2(x) \}^{1/2}. \quad (9)$$

Equation (9) represents a simple linear coupling of two modes, corresponding to the phonon and the configurational change. The lower branch ω_- will be required to vanish at $x=0.2$, where the $T1$ to $T2$ transition is observed to occur. Since the transition is driven by the configuration change, rather than phonon condensation, we have the condition $x_0 < x_c \lesssim 0.2$. It is convenient to define two limits, that of strong coupling [$V(x) \geq c$] and that of weak coupling [$V(x) \ll c$]. The two branches given by Eq. (9) are plotted in Fig. 4 vs x for both cases. The residues of $D(\omega)$ at ω_{\pm} are given by

$$A_{\pm} = \text{Res } D(\omega_{\pm})$$

$$= \frac{1}{2} \left(1 \pm \frac{c(x-x_0)^{1/2} - \epsilon(x-x_c)}{\{[c(x-x_0)^{1/2} - \epsilon(x-x_c)]^2 + 4V^2(x)\}^{1/2}} \right). \quad (10)$$

A_{\pm} determines the amount of phonon character at ω_{\pm} and is also shown in Fig. 4. The results of the coupling are that the phonon softening is suppressed near $x=0.2$, and that the amount of phonon character in the ω_{-} mode near $x=0.2$ in the weak-coupling case is very small. This is to be expected, since it is the configuration change, and not the soft phonon, which drives the transition.

IV. ELECTRONIC STRUCTURE

The electronic structure of $M_x\text{WO}_3$ for M an alkali metal can be considered as analogous to that of SrTiO_3 for $x=0$ and ReO_3 for $x=1$. These materials possess the same number of electrons/unit cell as WO_3 and $M\text{WO}_3$, respectively, and their band structures have been calculated.^{16,17} Within a rigid-band model, one can then view the increase of x in $M_x\text{WO}_3$ in terms of the addition of electrons to the ReO_3 conduction band calculated by Mattheiss.¹⁷ This band is derived from overlap between the t_{2g} d orbitals of the transition-metal ion and the p orbitals of the oxygen. Wolfram has shown¹⁸ that the planar nature of the overlap results in a dependence of the t_{2g} conduction-band energy on only two components of the wave vector. This leads to characteristic structure, such as a very rapid rise in the density of states at the band edge, which in the simple analytic approximation used in Ref. 18 is a discontinuity, and a very sharp peak near the center of the band, which in the simple analytic approximation is a logarithmic singularity. As a result of these features the rigid-band model for $M_x\text{WO}_3$ would predict a more rapid rise of $N(0)$ with x than the $x^{1/3}$ which would result from the usual $E^{1/2}$ band edge. Using the analytic expression for the t_{2g} -band Green's function given in Ref. 18, one can compute $N(0)$ vs x for $M_x\text{WO}_3$, within the rigid-band model and assuming that the Fermi level for $x=1$ is that appropriate to ReO_3 (Ref. 17). The result is that $N(0)$ is linear in x over a wide range, but with very small slope, and a reasonably large intercept, so that within the $T1$ phase ($0.2 < x < 0.4$) $N(0)$ would be almost constant. Recent calculations¹⁹ of the band structure of NaWO_3 yield some differences from the ReO_3 case, and the rigid-band model for Na_xWO_3 using these results also gives a linear relation between $N(0)$ and x , but with larger slope and smaller intercept.

The experimental data on both specific heat and susceptibility of cubic Na_xWO_3 suggest³ that $N(0)$ is indeed linear in x , but with practically zero intercept. Preliminary susceptibility measurements in the $T1$ phase also show this behavior.²⁰ In addition, recent x-ray photoemission studies²¹ of cubic

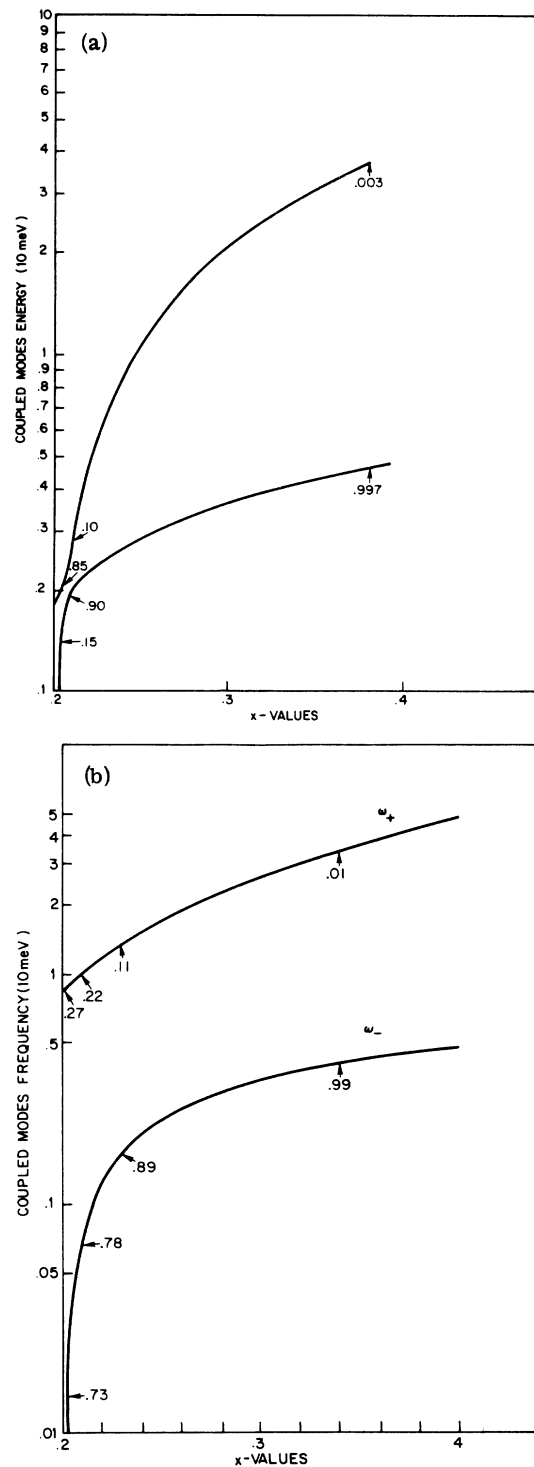


FIG. 4. Coupled modes described by Eq. (9): (a) corresponds to $x_0=0.17$, $x_c=0.1975$, $V_0=0.19$ meV, $\xi=10$, $c=10$ meV, $\epsilon=200$ meV, the weak-coupling limit. (b) corresponds to $x_0=0.14$, $x_c=0.17$, $V_0=3.8$ meV, $\xi=1$, $c=10$ meV, $\epsilon=200$ meV, the strong-coupling limit. The numbers above and below the curves indicate the amount of phonon character to the mode. The coupled modes depend little on the choice of ξ from $\xi=1$ to $\xi=10$.

Na_xWO_3 are in essential agreement with predictions based upon the filling of a t_{2g} band, similar to that of ReO_3 , by electrons donated by the sodium.

In the following we will treat the density of states as linear in x , as observed experimentally.^{3,20} We will also neglect any variation with x of the electron-phonon matrix element. The rationale for this last assumption is that the rigid-band model based on the characteristic shape of the t_{2g} conduction band in the d -band perovskites seems to account for several features of the experiments^{3,20,21} on Na_xWO_3 . We thus feel that it is unlikely that the electron-phonon matrix element would vary strongly with x , since such variation would imply large changes with x in the electronic wavefunctions as well, and the discussion above suggests that this is not the case. We also restrict our treatment to the metallic phases ($x > 0.2$), and do not consider the metal-semiconductor transition.

V. SUPERCONDUCTING TRANSITION TEMPERATURE

In Sec. III, we calculated the x dependence of the soft-phonon frequency, taking into account the important effects of the configuration coupling near the T_1 - T_2 transition. We now investigate the effect of this dependence on the superconducting transition temperature in the T_1 phase, assuming that this phonon makes the major contribution to the variation of T_c with x . For this purpose, we will utilize McMillan's formulation²² of T_c in terms of the electron-phonon spectral function $\alpha^2 F(\omega)$. According to Ref. 22

$$T_c = \frac{\langle \omega \rangle}{1.2} e^{-\left(\frac{1.04(1+\lambda)}{\lambda - \mu^* - 0.62\lambda\mu^*} \right)}, \quad (11)$$

where μ^* is the Coulomb pseudopotential,

$$\lambda = 2 \int_0^\infty \frac{\alpha^2 F(\omega) d\omega}{\omega}, \quad (12a)$$

$$\langle \omega \rangle = \frac{2}{\lambda} \int_0^\infty \alpha^2 F(\omega) d\omega, \quad (12b)$$

and $\alpha^2 F(\omega)$ is defined by²³

$$\alpha^2 F(\omega) \equiv \left(-\frac{1}{\pi} \sum_{\vec{k}, \vec{Q}} |M(\vec{k} - \vec{k} + \vec{Q})|^2 \text{Im} D(\vec{Q}, \omega) \right) \times \delta(\epsilon_{\vec{k} + \vec{Q}}) \delta(\epsilon_{\vec{k}}) / \sum_{\vec{k}} \delta(\epsilon_{\vec{k}}). \quad (13)$$

In Eq. (13) M is the matrix element for an electron-phonon scattering to occur between electron states \vec{k} and $\vec{k} + \vec{Q}$ on the Fermi surface, and $D(\vec{Q}, \omega)$ is the propagator for a phonon of momentum \vec{Q} . Assuming, as explained in Sec. IV, that $N(0) \sim x$, and M is independent of x , and taking²⁴ $\mu^* = 0.15x$, we obtain for the x dependence of λ and $\langle \omega \rangle$

$$\lambda = \frac{\alpha x}{(x - x_0)^{1/2}} \left(\frac{A_+}{\omega_+} + \frac{A_-}{\omega_-} \right), \quad (14a)$$

$$\langle \omega \rangle = \beta (A_+/\omega_+ + A_-/\omega_-)^{-1}, \quad (14b)$$

where α and β are constants, and ω_+ , ω_- , A_+ , and A_- are derived in Sec. III. For x not too close to 0.2, $A_- \sim 1$, $A_+ \sim 0$, $\omega_- \sim \omega_0 = c(x - x_0)^{1/2}$, so that (neglecting for the moment μ^* and noting that $\lambda \ll 1$), T_c will be of the form

$$T_c(x) = A(x - x_0)^{1/2} e^{B/x} \quad (x \gg 0.2). \quad (15)$$

This is the prediction of a simple soft-phonon model, neglecting the configurational tunneling. Since the tunneling will decrease in importance as x increases and one moves further from the T_1 - T_2 phase boundary, we expect Eq. (15) to be a good approximation at the high end of the range $0.2 < x < 0.4$. Consequently, we have plotted in Fig. 5 Shanks's data³ on $T_c(x)$ for sodium tungsten bronze along with Eq. (15), with A and B determined by fitting to the two highest x data points, and for several values of x_0 . The curves are both independent of x_0 and seem to fit the data reasonably well until one gets much below $x = 0.3$. For values of x very near the T_1 - T_2 boundary ($x = 0.2$), however, Eq. (15), for these values of A and B , and any x_0 , is seen to seriously overestimate the enhancement of T_c . We have also studied the effect of changes in the constants A and B on the fits, and find that for no values of the parameters can one obtain a good fit to the Shanks's data for the full range $0.2 < x < 0.4$ with Eq. (15). We do feel, however, that the physically most reasonable procedure is to use the high- x data to determine A and B , as in Fig. 5, since Eq. (15) is expected to be valid for x far from 0.2.

It is precisely in the region of x near 0.2 that the configurational tunneling becomes important, so that to understand the variation of T_c with x in this region one must go back to Eq. (14), and include the phonon-configuration coupling. The effect of this coupling will be to suppress somewhat the strong enhancement of T_c obtained from the bare soft phonon near $x = 0.2$, as can be seen from Fig. 4, where the phonon softening is suppressed by the configurational tunneling mode. In Fig. 6, we show numerical results for $T_c(x)$ vs x with the same sets of values of the parameters as in Fig. 4. The configuration-phonon coupling indeed suppresses the enhancement of T_c . In addition a maximum value of T_c is obtained. In the weak-coupling limit, Fig. 6(a), this maximum occurs very close to the transitional composition, is not shown, and may not be observable. The choice of parameters of Fig. 6(a) gives good agreement with the data of Ref. 3 for the T_1 - T_2 transition in Na_xWO_3 . In the strong-coupling case, shown in Fig. 6(b) $T_c(x)$ vs x develops a pronounced maximum for x significantly larger than the critical value (assumed here to be $x = 0.2$). One might speculate that the reason for the weak-coupling behavior in the sodium case is that since

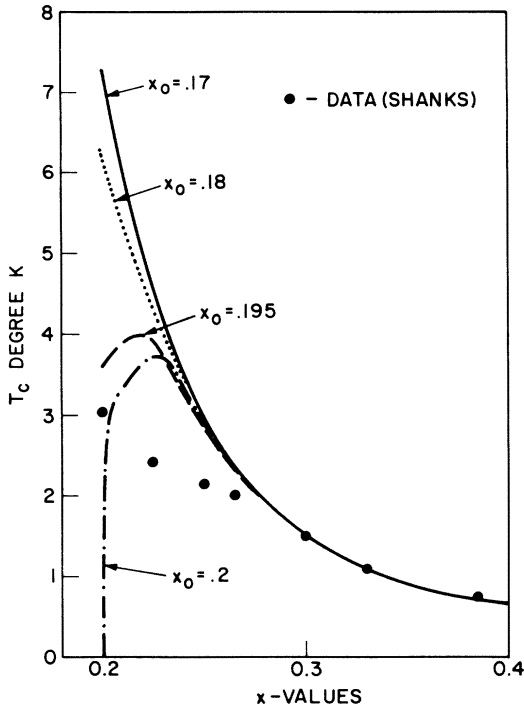


FIG. 5. Numerical evaluation of Eq. (15) and the data of Ref. 3 vs x . Parameters A and B in Eq. (15) are determined by fitting the high- x end of the data points.

T_2 is the most favorable configuration for the WO_6 octahedra alone, the barrier illustrated in Fig. 3 should be large. For transitions between two distorted phases, such as T_1 and hexagonal for example, the barrier should be smaller due to the fact that the WO_6 free energies of the two phases are almost the same: Thus the strong-coupling behavior illustrated in Fig. 6(b) might be expected for transitions not involving the T_2 or cubic phases.²⁵

VI. CONCLUSIONS

We have treated the T_1 - T_2 phase transition in sodium tungsten bronze with a two-well configuration-space model for the free energy. Tunneling between the configurations is allowed via a particular phonon, which softens as x approaches the critical composition. Since the change in configurations involves a change in the bonding, the transition is not accomplished simply by the condensation of the soft phonon as, for example, in the case of the Peierls transition²⁶ or the usual anharmonic soft phonon.⁶ Moreover, the phonon softening is obtained here even in the harmonic approximation, since the force constants depend upon x .¹² An interesting feature of the tungsten bronze system is that since the phonon softening occurs as a function of composition rather than temperature, it is possible to have the superconducting transition and

lattice instability occur simultaneously. Also, since the phonon involved is essentially a localized excitation, it has a greater effect on T_c than a soft mode with a particular wave vector. In the latter case only a small fraction of the phonon density of states is involved in the enhancement of the electron-phonon interaction.

We have utilized a simple model of both the soft

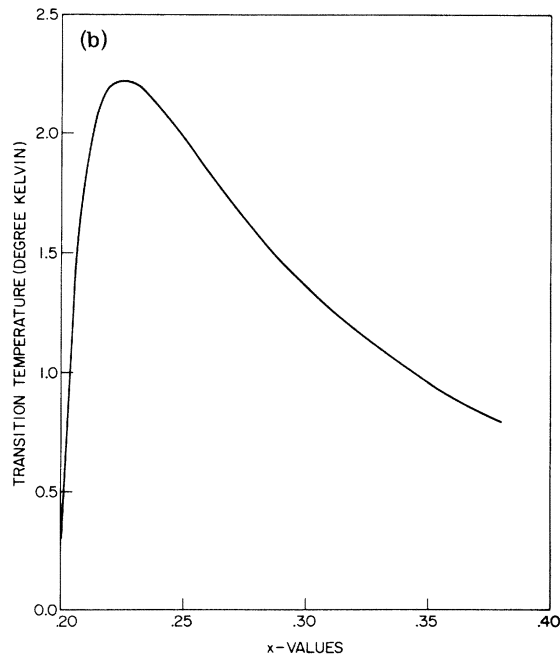
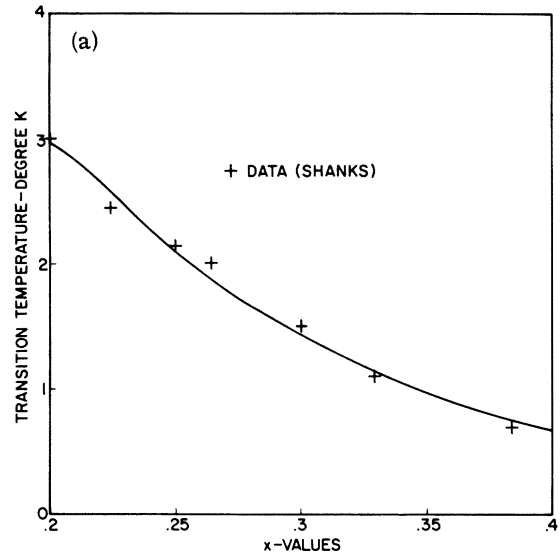


FIG. 6. Numerical evaluations of Eq. (11) for the sets of parameters used in Fig. 4. (a) Weak coupling as in Fig. 4(a), and (b) strong coupling as in Fig. 4(b). Data points in (a) are again taken from Ref. 3. The results depend little on the choice of ξ from $\xi = 1$ to $\xi = 10$.

phonon itself and of the phonon-configuration coupling, and included the effects of this coupling very near the transition. Within the simple model we have explicitly calculated the dependence of T_c on x , and have obtained good agreement with the data of Ref. 3 on Na_xWO_3 . As x is decreased toward the critical composition, the phonon softening enhances T_c dramatically, but this softening is suppressed by the phonon-configuration coupling very near the transition, and T_c then increases more slowly, exhibiting a visible maximum in the strong-coupling case.

It should be noted that our model is a semiempirical one, containing several parameters and assumed functional forms, and that there is at present a limited amount of data with which to make comparisons. For this reason, the good agreement between theory and experiment displayed above should not be construed as a definitive confirmation of the model. We rather view this as a demonstration of the correctness of the gross physical features of our picture of compositionally-dependent mode softening, as applied to Na_xWO_3 . Detailed confirmation of particular features of the model, such as the x dependence of ω_0^2 , or the importance of configurational tunneling, must await further experiments.

A direct observation of compositionally dependent mode softening in the tungsten bronzes is of great interest and importance at the present time. Earlier Raman scattering studies²⁷ of metallic tungsten bronzes were restricted to the higher frequency range. While either light scattering or ul-

trasonic attenuation and dispersion measurements can in principle yield the desired information, there are technical difficulties in performing these experiments on alkali tungsten bronzes. Perhaps the best opportunity is afforded by inelastic neutron scattering. Indeed, the phonon spectrum of hexagonal K_xWO_3 has already been measured²⁸ with neutrons for $x=0.33$ at room temperature. The results show three regions of the phonon spectrum with extremely flat dispersion. One of these corresponds to motions of atoms at opposite sides of the unit cell in opposite directions in the a - b plane, and would, in the $T1$ phase, lead to a shear force which could produce the rotation of octahedra illustrated in Fig. 2. Clearly these inelastic-neutron-scattering experiments should be extended to lower values of x , and into the $T1$ phase. The results of our calculations strongly suggest that softening of the phonon spectra should be observed.

ACKNOWLEDGMENTS

The authors are grateful to Dr. N. J. Chesser and Dr. A. J. Sweedler, and Professor H. Ehrenreich, Professor A. B. Harris, Professor D. J. Scalapino, Professor J. R. Schrieffer, Professor H. Shanks, and Professor T. Wolfram for helpful discussions of this work, and to Mrs. Bertha W. Hennis for assistance with the numerical calculations. One of us (R. S.) expresses his appreciation to the Naval Research Laboratory, where much of this work was performed, and to the Aspen Center for Physics, where the original draft of the manuscript was written, for their generous hospitality.

¹A. D. Wadsley, in *Non-Stoichiometric Compounds*, edited by L. Mandelcorn (Academic, New York, 1964).

²C. J. Raub, A. R. Sweedler, M. A. Jensen, S. Broadsten, and B. T. Matthias, *Phys. Rev. Lett.* **13**, 746 (1964); A. R. Sweedler, C. J. Raub, and B. T. Matthias, *Phys. Lett.* **15**, 108 (1965); J. P. Remeika, T. H. Geballe, B. T. Matthias, A. S. Cooper, G. W. Hall, and E. M. Kelly, *Phys. Lett. A* **24**, 565 (1967).

³H. R. Shanks, *Solid State Commun.* **15**, 753 (1974).

⁴B. C. Hyde and M. O'Keefe, *Acta Crystallogr. A* **29**, 243 (1973).

⁵P. W. Anderson, B. I. Halperin, and C. Varma, *Philos. Mag.* **25**, 1 (1972).

⁶W. Cochran, *Adv. Phys.* **9**, 387 (1960); P. W. Anderson, *Fiz. Dielect.*, edited by G. I. Skanawi (Academy of Sciences, Moscow, 1960).

⁷A. J. Bevelo, H. R. Shanks, P. H. Sidles, and G. C. Danielson, *Phys. Rev. B* **9**, 3220 (1974).

⁸J. C. Slater, *Quantum Theory of Molecules and Solids* (McGraw-Hill, New York, 1965), Vol. 2.

⁹H. R. Shanks, *Cryst. Growth* **13/14**, 433 (1972).

¹⁰Since the triangular tunnels are too small to contain M atoms, the $T1$ configuration has available per unit cell one square tunnel and four pentagonal ones, whereas $T2$ has nine squares. The outer tunnels are shared with

other unit cells, so the ratio becomes 3:5, hence $x_{\max}(T1) = 0.6$.

¹¹The hexagonal phase consists of only triangular and hexagonal tunnels (see Ref. 1, p. 139), and thus cannot be derived geometrically from $T2$ in the same manner as $T1$. The free-energy arguments made in the text are nonetheless valid for this phase.

¹²Equation (4) assumes uncorrelated behavior of the M atoms. We note that a linear dependence of ω^2 on x has been observed for a TO phonon in the nonstoichiometric ferroelectric PZT by G. Burns and B. A. Scott [*Phys. Rev. Lett.* **25**, 1191 (1970)], as described in A. Pinczuk, *Solid State Commun.* **12**, 1035 (1973).

¹³J. Cowley (private communication).

¹⁴Contributions from all possible configurational paths between $T1$ and $T2$, or from all combinations of phases of rotating groups of WO_6 octahedra, are included in the tunneling matrix element $V(x)$.

¹⁵A. A. Abrikosov, L. P. Gorkov, and I. E. Dzyaloshinskii, *Quantum Field Theoretical Methods in Statistical Physics*, 2nd ed. (Pergamon, New York, 1965).

¹⁶A. H. Kahn and A. J. Leyendecker, *Phys. Rev.* **135**, A1321 (1964).

¹⁷L. F. Mattheiss, *Phys. Rev.* **181**, 987 (1969); **B** **2**, 3918 (1970).

- ¹⁸T. Wolfram, Phys. Rev. Lett. 29, 1383 (1972).
- ¹⁹S. H. Liu (private communication).
- ²⁰H. Shanks (private communication).
- ²¹M. Campagna, G. K. Wertheim, H. R. Shanks, F. Zumsteg, and E. Banks, Phys. Rev. Lett. 34, 738 (1975).
- ²²W. L. McMillan, Phys. Rev. 167, 331 (1968). The general form of this equation can be derived analytically from the Eliashberg gap equations, although to obtain the constants numerical calculations based on the phonon spectrum of *Nb* were used. The results obtained in this paper do not depend on the exact values of these constants.
- ²³D. J. Scalapino, in *Superconductivity*, edited by R. D. Parks (Dekker, New York, 1969).
- ²⁴This assumes that the density of states dominates the Coulomb pseudopotential, and gives for $x=1$ a value close to that predicted by the nearly free electron model and observed in many metals.
- ²⁵There is some evidence that $T_c(x)$ in the hexagonal phases of K_xWO_3 and Rb_xWO_3 behaves in this fashion: H. J. Shanks (private communication) and D. R. Wanlass and M. J. Sienko, J. Solid State Chem. 12, 362 (1975).
- ²⁶M. J. Rice and S. Strassler, Solid State Commun. 13, 125 (1973); P. A. Lee, T. M. Rice, and P. W. Anderson, *ibid.* 14, 703 (1974).
- ²⁷J. F. Scott, R. F. Leheny, J. P. Remeika, and A. R. Sweedler, Phys. Rev. B 2, 3883 (1970).
- ²⁸N. J. Chesser (private communication).